Polymer inclusion membranes based on CTA/PBAT blend containing Aliquat 336 as extractant for removal of Cr(VI): Efficiency, stability and selectivity

Ferhat Sellami, Ounissa Kebiche-Senhadji, Stéphane Marais, Nicolas Couvrat, Kateryna Fatyeyeva

Polymer inclusion membranes based on CTA/PBAT blend containing Aliquat 336 as extractant for removal of Cr(VI): efficiency, stability and selectivity

Ferhat Sellami[1,2], Ounissa Kebiche-Senhadji[1], Stéphane Marais[2], Nicolas Couvrat[3], Kateryna Fatyeyeva[2*]

[1]*Laboratoire de procédés membranaires et de technique de séparation et de récupération (LPMSTR), Université A. Mira de Bejaia, Targa Ouzemmour 06000, Bejaia, Algeria*

[2]*Normandie Univ., UNIROUEN, INSA ROUEN, CNRS, PBS, 76000 Rouen, France*

[3]*Normandie Univ., UNIROUEN, INSA ROUEN, CNRS, SMS, 76000 Rouen, Franc*

*corresponding author: kateryna.fatyeyeva@univ-rouen.fr

Abstract

Cellulose triacetate (CTA) and poly(butylene adipate-*co*-terephthalate) (PBAT)-based polymer inclusion membranes (PIMs) containing ionic liquid (tricaprylmethylammonium chloride (Aliquat 336)) as the carrier extractant were obtained for the facilitated and selective transport of Cr(VI) ions. The composition of PIMs was optimized in terms of the CTA/PBAT ratio. The obtained membranes were investigated using different techniques in order to show the influence of the membrane composition and the ionic liquid presence on the PIM resulting properties. The infrared analysis confirmed the presence of the intermolecular interactions of the hydroxyl groups of CTA with the carboxyl groups of PBAT and of the negatively charged carboxyl groups of CTA with the positively charged ammonium groups of Aliquat 336. The water contact angle measurements highlighted that the Aliquat 336 and PBAT presence modified the membrane hydrophobic/hydrophilic character. Moreover, it was shown that PIM containing the equivalent content of CTA and PBAT (35/35 wt.%/wt.%) with 30 wt.% of Aliquat 336 revealed the optimized composition and was used for the Cr(VI) ions transport measurements. It was found that this PIM transported more than 99% of Cr(VI) in only 6h and accumulated less than 5% of Cr(VI) ions with a high initial flux. For the first time it is shown that the selective Cr(VI) transport through blend PIM with reduced extractant content and without plasticizer is more efficient compared to common PIMs. Besides, the stability of obtained blend PIMs was confirmed by carrying out continuous transport studies over a long period of time (more than 120h).

Keywords: polymer inclusion membrane, CTA, PBAT, Aliquat 336, Cr(VI) extraction.

1. Introduction

The heavy metal pollution is among the world's most alarming environmental problems whereby more than 95 million people are affected. The top six toxicants in 2017 were lead, radionuclides, mercury, hexavalent chromium, pesticides and cadmium. Hexavalent chromium (Cr(VI)) ion is one of the heavy metal ions with a high toxicity even in very low concentrations. Cr(VI) causes DNA damage [1], it is carcinogenic [2], and mutagenic in human cells [3]. In aqueous solution, Cr(VI) ions exist in the form of oxyanions such as $HCrO_4^-$ and $Cr_2O_4^{2-}$ which depend on the pH value. Cr(VI) is widely used in various branches of industry, such as electroplating [4], leather tanning [5], and textile [6]. Hence, the effluents from these industries are the major source of the Cr(VI) pollution. Several methods, such as the liquid extraction [7], chemical precipitation [8], electrodialysis [9], photocatalysis [10] and membrane filtration [11, 12], have been developed to remove Cr(VI) ions from water. However, these methods have several disadvantages including the requirement of large amounts of the organic solvent, high cost and the fact that they are far from being ideal for the technical application. For example, adsorption has been a widely used technique to remove not only Cr(VI) ions, but also other hazardous substances from water [12]. Many investigations have been carried out for the development of the adsorbents and their application towards the Cr(VI) extraction [13]. However, adsorption has a limitation in the recollection of the adsorbent after its binding with Cr(VI) and a risk of the secondary pollution with the adsorbent itself.

Among different membrane technologies, the liquid membranes have acquired a prominent role for their use in the separation, purification or other analytical applications, such as biomedicine, ion selective electrodes, effluent treatment and hydrometallurgy [14]. The application of the liquid membrane in the separation processes has increased significantly in recent years. The major importance of the membrane separation technology lies essentially in the fact that it is potentially energy-efficient and the membranes are highly permeable and highly selective. Separation systems have recently attracted much attention because of their lower cost and greater flexibility. There are several main types of the liquid membranes, namely bulk liquid membrane (BLM), emulsion liquid membrane (ELM), supported liquid membrane (SLM) and polymer inclusion membrane (PIM). SLM extraction process can selectively remove the specific compound in a single step and, hence, it has great potential for the large scale application [14]. Also, it is an alternative to the conventional solvent extraction

because of its high selectivity, operational simplicity, low solvent inventory, low energy consumption and zero effluent discharge [15]. However, it has a main drawback which is a lack of the long-term stability [16].

In recent years, PIMs have proved to have properties making them extremely attractive for the application in a wide range of the separation processes [17]. The interest of this type of membranes is mainly due to their higher stability compared to that of SLMs. Besides retaining most advantages of SLM, PIM contains effective carrier and it is easy to prepare, is versatile and stable, and has good chemical and mechanical properties compared to SLM.

PIMs are formed by casting a solution containing a base polymer, an extractant (carrier) and a plasticizer. The base polymer such as poly(vinyl chloride) (PVC) or cellulose triacetate (CTA) forms a thin, flexible and stable film ensuring the mechanical strength. The extractant effectively transports and binds the ion across the membrane, and plasticizers are additives that increase the plasticity or fluidity of the final material. In general, the plasticizers are the organic compounds containing a hydrophobic alkyl backbone and one or several highly solvating polar groups. The softening action of the plasticizers, so called plasticization, is usually attributed to their ability to reduce the intermolecular attractive forces between the polymer chains. In addition to the improvement of the membrane flexibility, the plasticizer improves also the compatibility between the membrane components (namely, the base polymer, carrier and carrier/extracted species complex or ion-pair) [18] and the permeability properties while increasing the metal species flux [19]. 2-Nitrophenyl octyl ether (NPOE) and 2-nitrophenyl pentyl ether (NPPE) are the most frequently used plasticizers and several studies have shown that PIMs with these plasticizers have exhibited higher initial flux values compared to the membranes containing other plasticizers [17, 18].

The resulting supporting PIM can selectively separate the solutes of interest in the way similar to that of SLM [18], but with higher performances as it contains a liquid extractant which acts as a carrier. The carrier is held within the membrane polymer structure instead of being dissolved in a diluent and held by the capillary forces within the relatively large pores of a polymer support as in the case of SLM, thus inhibiting the carrier leaching [20]. This fact proves that PIM has a longer lifetime and greater stability than SLM in respect to the loss of the membrane liquid phase to the aqueous phase [11, 13, 18].

During the last decades there appears a large number of articles devoted to PIMs that shows a great interest in this kind of membranes. It was found that the transport mechanism in PIM depended on different factors, such as the membrane composition, homogeneity as well

as the surface morphology [15, 18, 20]. Often PIMs do not incorporate a plasticizer as a number of carriers, such as quaternary ammonium salts and phosphoric acid esters, have already plasticizing effects [21].

Recently, ionic liquids (ILs) have shown good performance as an extractant phase in the separation of the heavy metal ions [18, 20, 22, 23]. ILs are low melting point salts, mostly obtained by the use of the bulky asymmetric cations and weakly coordinating anions. Tailoring the length and branching of the alkyl chains on the cations and anions can be used to produce task specific ILs. Besides, IL can be considered as a carrier and a plasticizer at the same time [22-24]. For example, Güell et al. have shown that PIM based on CTA and containing 47.6% of tricaprylmethylammonium chloride (Aliquat 336) offers the highest efficiency for the As(V) removal compared to the membranes with different compositions including the membranes containing NPOE [21]. However, the concentration of the carrier in this case is still rather high (50%) and cannot be lowered without the membrane performance decrease.

PVC and CTA are still the most widely used base polymers for PIMs, since they provide the high mechanical strength and are compatible with most used carriers [18]. However, in addition to PVC and CTA, other polymers have been also tested. Gardner et al. studied the effect of the size of the polymer side chain on the ion transport across the membranes using cellulose acetate propionate (CAP), cellulose acetate butyrate (CAB) and cellulose tributyrate (CTB) using bis-*tert*-butylcyclohexano-18-crown-6 as the metal cation carrier [25]. They observed that the ion transport through the membrane decreased with the polymer alkyl chain length increasing. On the other hand, Kebiche-Senhadji et al. compared PVC-based membranes containing Aliquat 336 with different PVC molecular weights for the Cr(VI) extraction and found that the molecular weight of the base polymer had only small influence on the membrane transport efficiency [26].

The research of developing biodegradable and eco-friendly polymers demanding less chemical treatment during production was on the rise last decades. Natural polymers have attracted researchers' attention to the waste water treatment, especially to the heavy metal removal, due to their physicochemical properties, economic viability, availability and the presence of various reactive groups on the backbone chain [27-29]. Poly(butylene adipate-*co*-terephthalate (PBAT) is a well-known biodegradable polymer [30]. It is a flexible material, which has a high elongation at break, as well as good hydrophilic and processing properties.

The polymer blends are developed when specific properties are required, taking into account that the properties of the multi-component polymer systems are influenced by the

nature of the polymers, their thermal behavior and their possible interactions. Thus, in the present work focused on the elaboration of new hybrid membranes (blend polymer inclusion membranes (BPIMs)), the influence of the polymer blend composition and the IL presence were studied in order to reveal the membrane efficiency for heavy metal removal applications. For this purpose, CTA and PBAT were chosen as the base polymers at different weight ratio due to the great compatibility of the aromatic polyesters [31]. In order to increase the separation efficiency of BPIMs, Aliquat 336 was used as extractant and was immobilized in the polymer membrane. The composition of BPIMs was optimized in terms of the membrane hydrophilicity. The effect of the membrane composition on the Cr(VI) transport properties was evaluated by permeation measurements.

2. Material and methods

2.1. Materials

CTA pellets with 43-49 wt.% acetyl and Aliquat 336 (≥ 97% purity) were received from Aldrich and used without further purification. PBAT or Ecoflex™ F Blend C1200 (M_w = 126 000 g/mol) was supplied by BASF in pellet form. Chloroform (99 – 99.4% purity) and hydrochloric acid were received from Sigma Aldrich. Sodium hydroxide (≥ 99% purity) and potassium chromate K_2CrO_4 (≥ 99.5% purity) were purchased from Merck and Acros organics, respectively. 1.5-diphenylcarbazide (DPC) (≥ 97% HPLC purity) was received from Fluka. All water used in the present work was milli-Q water (Milli-Q Water System, Millipore, resistivity = 18 MΩ/cm at 25 °C).

2.2. Membrane preparation

The polymer inclusion membranes based on CTA, PBAT or their mixture (CTA/PBAT) were prepared using a procedure similar to that reported by Annane et al. [32]. For this purpose, the required amounts of polymers were separately dissolved in chloroform at the concentration of 10 mg/mL for CTA and 100 mg/mL for PBAT at room temperature (24 ± 1 °C). The certain quantity of Aliquat 336 (30 wt.%) dissolved in 5 mL of chloroform was added to the blend polymer solution and the mixture was stirred during 30 min to obtain a homogenous solution. The final solution was poured in a 9.0 cm diameter covered glass Petri dish and the solvent was slowly evaporated during 72h at room temperature (24 ± 1 °C) and hygrometry (48 ± 2% of relative humidity). The resulting membrane was then carefully

peeled off from the bottom of the Petri dish and taken for further studies. The thickness of the free-standing membranes was 110 ± 5 µm.

For the membrane based on CTA and PBAT, different compositions were used. For the sake of clarity, XCTA/YPBAT/30Aliquat 336 refers to the membrane with a certain amount of CTA and PBAT and 30 wt.% Aliquat 336. The values of X and Y represent the CTA or PBAT amount, respectively, expressed in wt.%. For the membranes with ionic liquid, the total polymer and ionic liquid weights were maintained constant (70 wt.% and 30 wt.% for polymer and ionic liquid, respectively) and the CTA/PBAT ratio was varied (Table 1).

2.3. Physical and chemical characterization

2.3.1. Fourier transform infrared (FTIR) spectroscopy

The FTIR spectra of various studied membranes were recorded by means of Nicolet Avatar 360 spectrophotometer equipped with a Germanium Attenuated Total Reflectance (ATR) mode. 200 scans were collected for each measurement over the 4000-400 cm^{-1} spectral range with the 4 cm^{-1} resolution. All the FTIR spectra were analyzed using Omnic software (version 5.2a).

Table 1. The composition of the studied BPIMs.

Membrane	CTA content, wt.%	PBAT content, wt.%	Aliquat 336 content, wt.%
CTA	100	-	-
70CTA/30Aliquat 336	70	-	30
52.5CTA/17.5PBAT/30Aliquat 336	52.5	17.5	30
35CTA/35PBAT/30Aliquat 336	35	35	30
17.5CTA/52.5PBAT/30Aliquat 336	17.5	52.5	30
PBAT	-	100	-

2.3.2. Tensile tests

The tensile measurements were performed with an universal tensile machine (Instron 5543) with the 500 N load cell according to ISO 527-A. All tests were carried out at the crosshead speed of 1 mm/min at room temperature (24 ± 1 °C) and hygrometry (48 ± 2% of relative humidity). For each sample, minimum seven specimens were tested and the mean values of Young's modulus *E*, elongation at break and tensile strength were calculated.

2.3.3. Contact angle measurements

Water contact angle θ of the membranes was measured using a contact angle goniometer (Multiscop goniometer Optrel) equipped with the image-processing software CAM *via* the sessile drop technique. The volume of each water droplet was 2.3 µL and at least 8 spots for each membrane were randomly analyzed to yield an average value of the contact angle. The measurements were performed at room temperature (24 ± 1 °C).

2.3.4. Scanning microscopy (SEM) analysis

SEM was used to analyze the microstructure of the membrane surfaces (in contact with air and glass) and cross-section. For the observation of the cross-section, the membrane was freeze-fractured using liquid nitrogen and a small piece of the membrane was mounted on a SEM specimen holder and image analysis was performed in the environmental mode using HITACHI S4500 microscope.

2.3.5. Differential scanning calorimetry (DSC)

The DSC measurements were performed by using Polyma apparatus from Netzsch. All the experiments were carried out in an aluminum pan with pierced lid in the nitrogen atmosphere at the heating/cooling rate of 10 °C/min. Two scans were performed for each sample from -50 °C to 200 °C: the first scan in order to remove the thermal history of the membrane, and the second one – to measure the thermal transitions. The results were analyzed with Proteus software. For each membrane composition, minimum three specimens were tested and the mean values of thermal transitions were calculated.

2.3.6. Thermogravimetric analysis (TGA)

The thermal stability of the membranes was determined using a thermogravimetric analyzer STA PT1600 from Linseis. About 5 mg of each membrane sample was taken and heated from 30 °C to 600 °C at the heating rate of 10 °C/min under a nitrogen atmosphere. For each membrane composition, minimum three specimens were tested.

2.3.6. X-ray diffraction analysis

X-ray diffraction analysis (Bruker D8 Discover diffractometer) using a Co-Kα radiation (wavelength of 1.7889 Å) was applied for the microstructural characterization of the membranes. The analysis was performed within the 2θ range of 3-60° with a step size of 0.04° at room temperature (24 ± 1 °C). The diffraction patterns were deconvoluted into peaks and halos referring to crystalline and amorphous regions, respectively, using a Gaussian function from Origin® 9.0 and according to the two-phase model [33]. For each membrane composition, minimum three specimens were studied.

2.4. Transport studies

In order to study the Cr(VI) transport from the feed compartment (10 mg/L of Cr(VI) in 0.1 M HCl) to the stripping phase (0.1 M NaOH), the transport experiments were carried out in a two-compartment (250 mL) permeation cell made of polytetrafluoroethylene (PTFE). The exposed membrane area was 12.56 cm^2. The continuous stirring of the both compartments at 1000 rpm was maintained during the experiment. All experiments were carried out at room temperature (24 ± 1 °C). The samples were taken periodically from both compartments and the Cr(VI) concentration was monitored using an UV-Vis spectrometer (ThermoFisher Evolution 220). The samples were sufficiently small to ensure that the membrane remained covered with the aqueous feed and stripping solutions throughout the transport experiments. The Cr(VI) concentration was determined in an acidic medium at λ_{max} = 542 nm [26] due to the complexation reaction with DPC *via* the formation of the violet complex Cr(VI)-DPC. For each membrane composition, minimum five specimens were analyzed.

The permeability P and diffusion D coefficients, and flux J of the transport process through the membrane can be described by the mass transfer model developed by Danesi [19, 34]. This model derives from the Fick's diffusion law and takes into account the difference in the distribution ratio between the organic phase absorbed in the membrane and the aqueous feed solution of Cr(VI) K_d. As in our case the metal carrier is a basic extractant (i.e. long chain alkylamine), so the difference in the K_d values between the feed and stripping solutions is obtained by the concentration gradient of the counterion (Cl^-) which is accompanying the metal cation into the membrane.

Since the flux J can be correlated to the concentration variation C, the aqueous feed volume V and the membrane area A as follows:

$$J = -\frac{dC}{dt}\frac{V}{A} \tag{1}$$

and the permeability coefficient P is given by:

$$P = \frac{J}{C}. \tag{2}$$

So, the integrated flux can be calculated according to:

$$\ln(\frac{C}{C_0}) = -\frac{A}{V}Pt \tag{3}$$

where C_0 and C are the concentration of the metal ions in the feed phase at the initial time and selected time, respectively, in mg/L and t is the time in s. The dependence of $\ln(\frac{C}{C_0})$ versus time was linear, which was confirmed by the high values of the determination coefficient R^2 (> 0.98). The permeability coefficient P was calculated as follows:

$$P = \frac{V}{A}k, \tag{4}$$

where k is the slope of the $\ln(\frac{C}{C_0}) = f(t)$ curve and corresponds to the kinetic rate constant in s^{-1}. The initial flux J_i value (in mol/(m^2·s)) was derived from the P values by the following equation:

$$J_i = PC_0 \tag{5}$$

The removal, recovery and accumulation factors were calculated to describe the efficiency of the Cr(VI) transport as follows:

$$Removal\ factor = \frac{C_0 - C}{C_0} \cdot 100\% \tag{6}$$

$$Recovery\ factor = \frac{C_{stripping}}{C_0} \cdot 100\% \tag{7}$$

$$Accumulation\ factor = \frac{C_{membrane}}{C_0} \cdot 100\% \tag{8}$$

where $C_{stripping}$ and $C_{membrane}$ are the Cr(VI) concertation in the stripping phase and membrane phase, respectively.

The concentration of the metal ions (such as Cr(VI), Co(II), Cu(II), Zn(II), Ni(II), Pb(II), Fe(III), Cd(II)) during the selectivity study was determined by the inductively coupled plasma spectrometer (ICP, Thermo iCAP 7000 Series). The measurements were performed in triplicate for reproducibility.

3. Results and discussion

3.1. FTIR analysis

FTIR spectroscopy was used to give information about the chemical difference between the membranes. The FTIR spectra of the studied membranes of the different composition are shown in Fig. 1. The spectra of pure polymers (CTA and PBAT) as well as pure Aliquat 336 are given for comparison. As it can be observed from the FTIR spectrum of

the pure CTA membrane (Fig. 1, curve 1), the band located around 1743 cm^{-1} is assigned to the stretching vibration of the C=O group in CTA [35, 36]. The presence of the bands at 1228 cm^{-1} and 1045 cm^{-1} corresponds to the stretching vibration of the C-O bonds. The absorption band at 1367 cm^{-1} is attributed to the C-H bonds. The main characteristic IR peaks of pure PBAT (Fig. 1, curve 2) are located at 2954 cm^{-1} (the asymmetric stretching vibration of -CH_2-), 1712 cm^{-1} (the stretching vibration of the C-O groups), 1456 cm^{-1} (the stretching of the phenylene groups), 1409 cm^{-1} and 1395 cm^{-1} (the -CH_2- *trans*-plane bending vibration), 1270 cm^{-1} (the symmetric stretching vibration of the C-O groups), 1105 cm^{-1} (the C-O symmetric stretching vibration absorption), 1021 cm^{-1} and 727 cm^{-1} (the bending vibration absorption of the C-H groups of the phenylene ring) [37, 38]. The absorption bands at 2923 cm^{-1} and 2851 cm^{-1} assigned to the -CH_3 groups and at 1467 cm^{-1} and 1378 cm^{-1} attributed to the quaternary ammonium groups [39, 40] (Fig. 1, curve 3) are in accordance with the chemical structure of Aliquat 336.

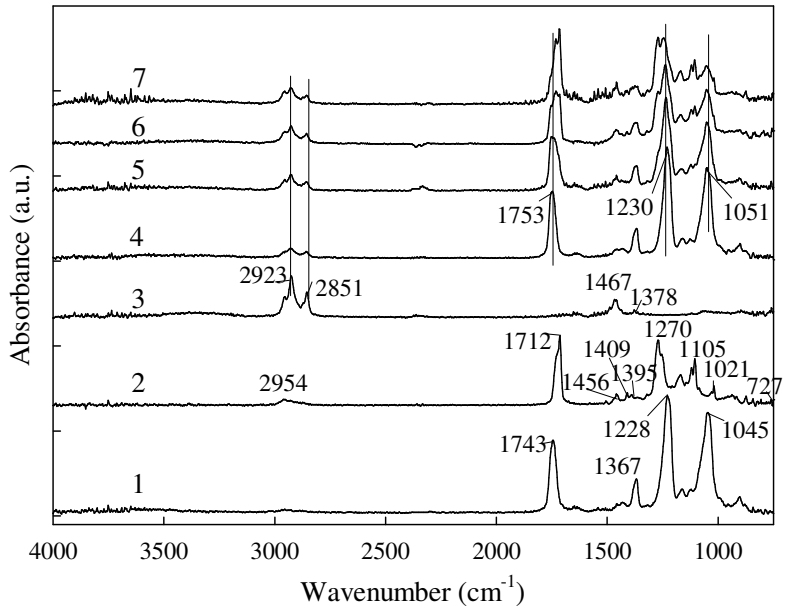

Figure 1. FTIR spectra of the obtained membranes: (*1*) CTA, (*2*) PBAT, (*3*) Aliquat 336, (*4*) 70CTA/30Aliquat 336, (*5*) 52.5CTA/17.5PBAT/30Aliquat 336, (*6*) 35CTA/35PBAT/30Aliquat 336, (*7*) 17.5CTA/52.5PBAT/30Aliquat 336.

In the case of the 70CTA/30Aliquat 336 membrane (Fig. 1, curve 4), the displacement of the absorption bands to the higher wavenumber region is observed. For example, the stretching vibration of the carbonyl groups is shifted from 1743 cm^{-1} to 1753 cm^{-1} and the absorption of the C-O bonds is observed at 1230 cm^{-1} and 1051 cm^{-1} instead of 1228 cm^{-1} and

1045 cm^{-1}, respectively. This shift is explained by the bond length decrease due to the intermolecular interaction of the functional polymer and ionic liquid groups [41-44]. In our case, this displacement to the higher wavenumbers is provoked by the interactions of the negatively charged carboxyl groups of CTA and positively charged ammonium groups of Aliquat 336. In addition, the shift of the carbonyl group vibration may testify to the membrane crystallinity changes [45].

For the polymer membranes based on CTA and PBAT, the similar spectral behaviour is noted, i.e. the shift of the characteristic absorption bands to the higher wavenumber region (Fig. 1, curves 5-7). The fact that the characteristic bands of both polymers and ionic liquid are present on the spectrum of BPIM as well as the fact that the band displacement is observed compared to the pure components allows us to assume that Aliquat 336 interacts with the polymer chains and, thus, may further interact with the species in the solution.

3.2. Hydrophilicity/hydrophobicity balance

The contact angle measurements are performed in order to examine the surface changes caused by the membrane composition as they are directly related to the membrane transport properties. The water contact angle values obtained for the pure CTA and PBAT membranes are 65±1° and 71±1°, respectively. Similar results were reported in the literature [20, 45]. When Aliquat 336 is added to the CTA membrane, the contact angle values decrease up to ~22° for the membrane containing 30 wt.% of ionic liquid (Fig. 2). This result is related

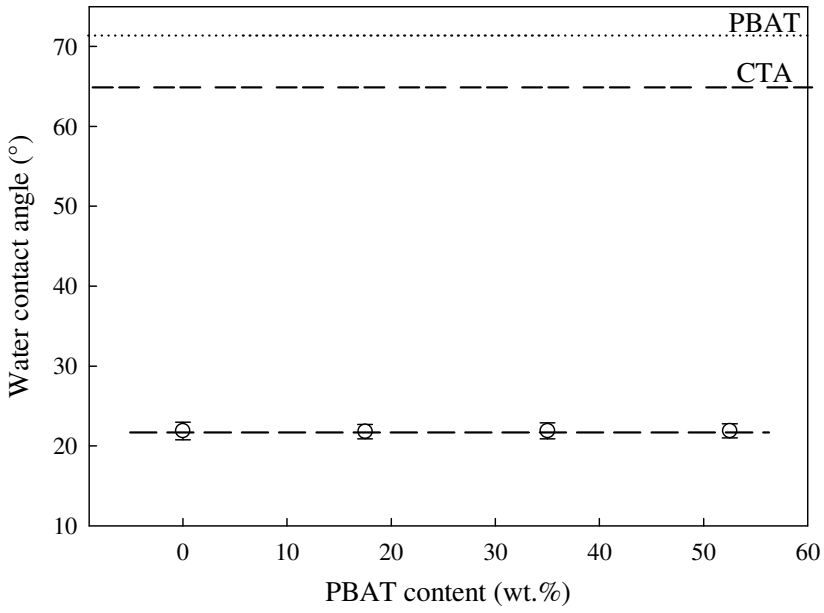

Figure 2. Water contact angle variation of CTA/PBAT/30Aliquat 336 membranes as a function of the PBAT content.

to the presence of the quaternary ammonium groups in Aliquat 336 as it is known that this group has highly hydrophilic property induced by the positively charged quaternary amine. It should be mentioned that the significant increase of the hydrophilic nature of BPIM is very favorable for the membrane transport properties [15, 18, 21].

In order to investigate the influence of the PBAT content on the hydrophilic/hydrophobic character of the CTA/PBAT/30Aliquat 336 membranes, the water contact angle measurements were carried out for the membranes with the same Aliquat 336 concentration (i.e. 30 wt.%) and polymer/ionic liquid ratio (i.e. 70 wt.%/30 wt.%) (Fig. 2). As one can see from the obtained results, no significant difference in the hydrophilic balance of the membranes is observed. Similar results were obtained in the case of the membranes based on PVC and CTA [23]. The authors found that the presence of Aliquat 336 modified strongly the membrane behavior from a hydrophobic character (86°) for the PVC membrane containing 9% Aliquat 336 to the hydrophilic (28°) character when the surface concentration of Aliquat 336 was higher than $1 \cdot 10^{-5}$ mol/cm^2. For the membranes with the Aliquat 336 concentration higher than 1.10^{-5} mol/cm^2, no influence of the polymer matrix composition on the hydrophilic/hydrophobic character was found.

3.3. SEM analysis

The membrane morphology plays a crucial role in determining the membrane properties. To investigate the influence of the membrane composition on the morphology, SEM images of the surface and cross-sections were collected. Fig. 3 presents the cross-section SEM images of the studied membranes. In the case of the pure CTA membrane, a smooth, compact surface was observed (Fig. 3a). When incorporating Aliquat 336, no significant changes were observed on the SEM image testifying to the compatibility of the polymer (CTA) and ionic liquid (Fig. 3b). In the case of BPIMs (Fig. 3c-e), homogeneous symmetric dense membranes were obtained as well. The membrane revealed pronounced facets typical of intergranular fracture in polycrystalline materials. Such a structure is presumably a consequence of the limited miscibility of the two polymers. However, no phase separation can be noticed that indicates a strong interfacial interaction between PBAT, CTA and Aliquat 336. Therefore, one may consider the obtained ternary blend to be miscible to some extent.

3.4. Mechanical properties

Generally, in order to improve the PIM flexibility and the compatibility of the membrane components (i.e. the base polymer and a carrier), a plasticizer is incorporated

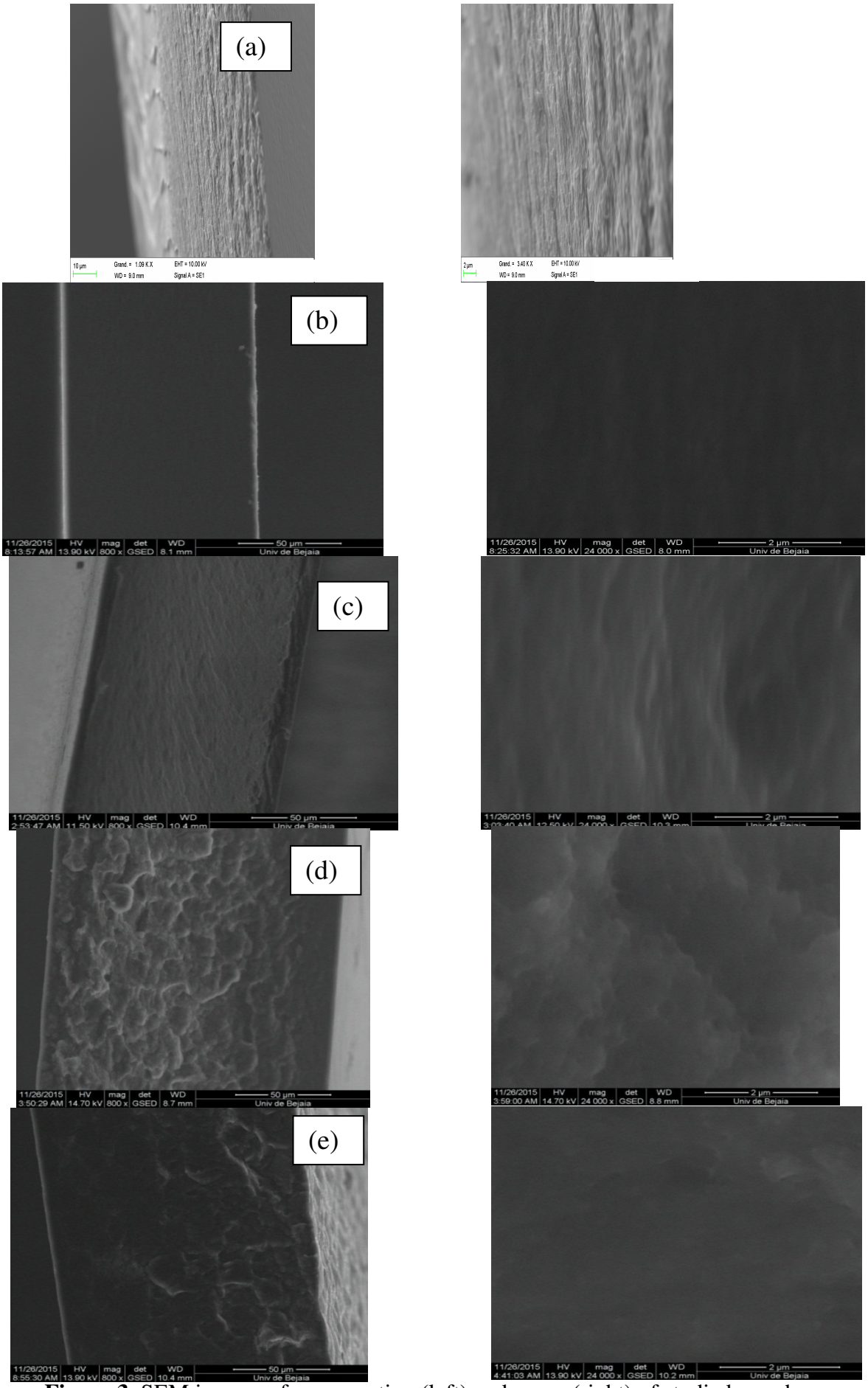

Figure 3. SEM images of cross section (left) and zoom (right) of studied membranes: (*a*) CTA, (*b*) 70CTA/30Aliquat 336, (*c*) 52.5CTA/17.5PBAT/30Aliquat 336, (*d*) 35CTA/35PBAT/30Aliquat 336, (*e*) 17.5CTA/52.5PBAT/Aliquat 336.

during the membrane preparation. The most commonly used plasticizers are NPOE and NPPE [18]. Recently it was shown that ionic liquids revealed an excellent additional plasticizing performance [23, 46].

The different membrane composition can be appreciated at a macroscopic scale when changes in the appearance and mechanical properties of the membranes are observed. The degree of crystallinity and the microstructure of BPIM are the main factors influencing the mechanical properties, which are very important for their viability in the separation application. Therefore, the stress-strain curves were measured and they are shown in Fig. 4a. It should be noted that previously performed measurements for the 70PBAT/30 Aliquat 336 membrane revealed very low mechanical properties of this membrane insufficient for the Cr(VI) removal.

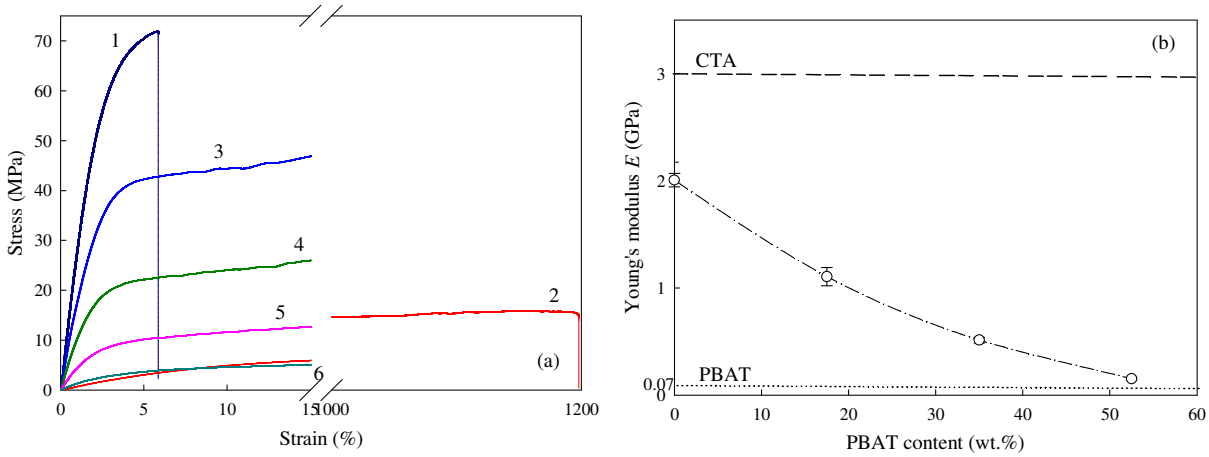

Figure 4. Representative stress-strain curves (*a*) and Young's modulus values (*b*) as a function of the membrane composition: (*1*) CTA, (*2*) PBAT, (*3*) 70CTA/30Aliquat 336, (*4*) 52.5CTA/17.5PBAT/30Aliquat 336, (*5*) 35CTA/35PBAT/30Aliquat 336, (*6*) 17.5CTA/52.5PBAT/30Aliquat 336.

As expected, two main characteristic zones are presented in the stress-strain curves (Fig. 4a) whatever the membrane composition. The first zone presents a linear behavior that corresponds to the elastic regime and the second zone presents a plastic behavior until the breaking point is reached. The Young's modulus E of the membrane can be determined from the slope of the linear zone at the beginning of the curve using Hooke's law:

$$\sigma = E \cdot \varepsilon, \tag{9}$$

where σ is the stress and ε is the strain. The results obtained for the Young's modulus values as a function of the PBAT content are shown in Fig. 4b.

In the case of the pure polymer membranes (CTA and PBAT) the Young's modulus values are 3.0 ± 0.1 GPa and 66.4 ± 2.0 MPa for CTA and PBAT, respectively (Fig. 4b). The large dispersity of the mechanical properties values may be found in the literature. For example, the Young's modulus value for the CTA membrane varies from 2 GPa [47] up to ~10 GPa [48]. This difference may be explained by the intrinsic properties of CTA, i.e. its molecular weight, degree of acetylation, etc. [49].

All the membranes prepared with Aliquat 336 present a higher elasticity than the membranes of pure polymers (i.e. CTA and PBAT). The addition of Aliquat 336 to the CTA membrane leads to the decrease of the Young's modulus value – 3.0 ± 0.1 GPa and 2.0 ± 0.1 GPa for the pure CTA membrane and the membrane containing 30 wt.% Aliquat 336, respectively (Fig. 4b). This result confirms the plasticizer effect of the ionic liquid.

The extremely high values of the Young's modulus can be understood as the result of the non-porous membrane structure (Fig. 3), which is compact, resulting in a more homogeneous stress distribution across the membrane that makes its deformation more difficult.

The increase of the PBAT content causes a decrease in the Young's modulus of around one order of magnitude (Fig. 4b) thus plasticizing the CTA/30Aliquat 336 membranes (also referred to as softening). C.-S. Wu reported the similar behavior of the maleic anhydride-grafted PBAT/cellulose acetate films [31]. In fact, the presence of the flexible chains of PBAT decreases the stiffness of BPIM compared to the 70CTA/30Aliquat 336 membrane. This chain mobility reduces the resistance to the mass transfer and facilitates the chain-segment movements.

3.5. Thermal characterization

The TGA curves presented in Fig. 5a refer to the pure CTA and PBAT membranes and BPIMs. The derivative thermogravimetric (DTG) curves (Fig. 5b) are given for better understanding the thermal behavior of the membranes. TGA measurements demonstrate that the pure CTA membrane is thermally stable until temperatures close to 350 °C. In the case of PBAT, the main degradation step is observed at approximately 390 °C. After this temperature, the carbon hydrogen bonds of the polymer chain break [36, 38].

The analysis of the obtained results shows the influence of the IL presence and membrane composition on the membrane degradation temperature. In the case of the 70CTA/30Aliquat 336 membrane the additional weight loss, which occurs at ~ 200 °C, is related to the ionic liquid decomposition. The Aliquat 336 addition clearly decreases the

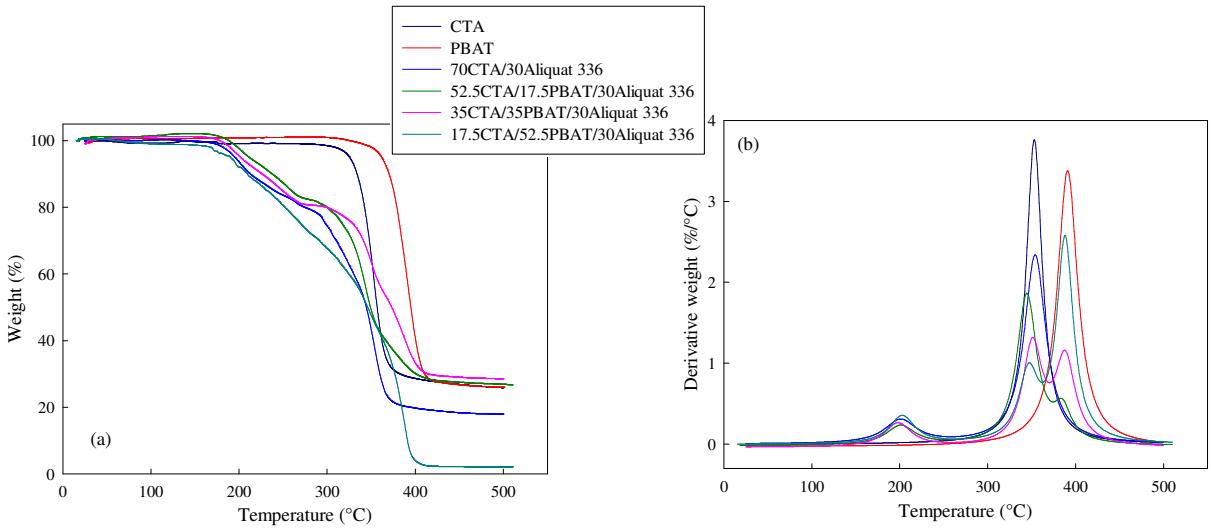

Figure 5. Thermogravimetrical (*a*) and DTG (*b*) curves of studied membranes.

degradation temperature of the CTA-based membranes. This fact suggests that the ionic liquid disrupts the polymer chain packaging, lowering the energy required to break the inter- and intra-bonding between the polymer chains, thus rendering them more labile [45]. It should be mentioned that the decomposition of Aliquat 336 starts before its melting point (225 °C). This result proves that Aliquat 336 has interacted with the macromolecular chains of CTA [49]. This observation is also in good agreement with the results of the FTIR analysis (Fig. 1) confirming the intermolecular interactions between Aliquat 336 and polymer chains.

In the case of the CTA/PBAT/30Aliquat 336 membranes, all thermal degradation curves are characterized by the three degradation steps (Fig. 5): the first weight loss step at ~ 200 °C corresponds to the Aliquat 336 decomposition, the second one at ~ 350 °C and the third one at ~ 400 °C are related to the CTA and PBAT degradation, respectively. It should be noted that the intensity of the peak at 200 °C (Fig. 5b) is practically the same for all membranes containing Aliquat 336 whatever the membrane composition, thus confirming the constant concentration of the ionic liquid in these membranes (30 wt.%).

Taking into account the obtained results, one can assume that obtained BPIMs are stable up to 150 °C (Fig. 5). Such thermal stability is quite sufficient for the membrane use in the separation at high temperatures without any risk of the membrane degradation or deterioration.

The thermal behavior of the membranes was also examined by the DSC analysis (Fig. 6) in order to study the miscibility, the possible interactions between the components of the polymer blends and the possible variations in phase transitions [50, 51]. It is well known that for a fully miscible polymer blend, a single glass transition temperature T_g value would be

obtained whereas for an immiscible polymer blend, more than one T_g value would be obtained. In addition, the DSC method makes it possible to evaluate the degree of crystallinity of a polymer X_c from the magnitude of the thermal effect corresponding to its melting process. This parameter defined as the ratio of the thermal effects of the sample under consideration and the theoretical fully crystallized polymer is calculated according to the following equation:

$$X_{C_{DSC}} = \frac{\Delta H_m - \Delta H_c}{\varphi \Delta H_m^{\circ}} \cdot 100\% \qquad (10)$$

where $X_{C_{DSC}}$ is the defined degree of crystallinity, ΔH_m corresponds to the melting heat of the membrane, ΔH_c is the enthalpy of cold crystallization, ΔH_m° is the melting heat of the 100% crystalline polymer and φ is the weight fraction of polymer in the blend membrane. The value of ΔH_m° for CTA has been estimated to be 58.8 J/g [33] and it is equal to 114 J/g for PBAT [52].

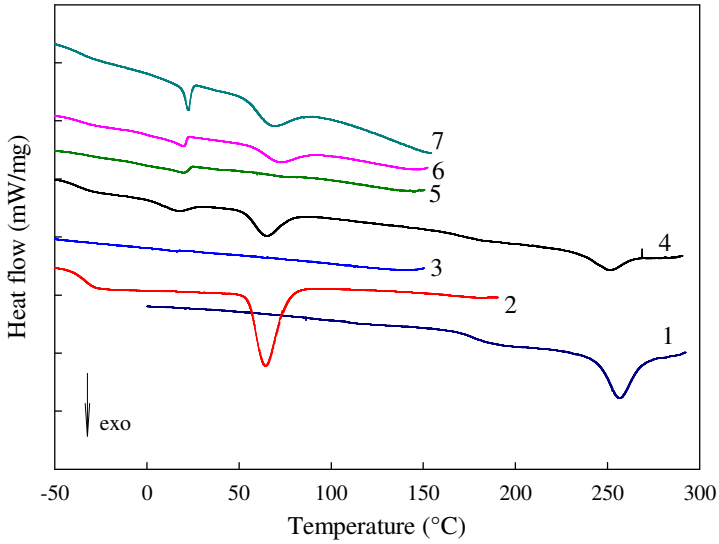

Figure 6. DSC curves of obtained: (*1*) CTA, (*2*) PBAT, (*3*) 70CTA/30Aliquat 336, (*4*) 50CTA/50PBAT, (*5*) 52.5CTA/17.5PBAT/30Aliquat 336, (*6*) 35CTA/35PBAT/30Aliquat 336, (*7*) 17.5CTA/52.5PBAT/30Aliquat 336.

The first cooling scan of the DSC thermograms of the pure CTA and PBAT membranes as well as those of BPIMs are given in Fig. 6. The T_g midpoint value for CTA was observed at 199.3 °C and that of PBAT – at -31.7 °C which is in good agreement with the literature data [37, 45, 53]. The crystallinity degree of the membranes determined from the first heating scan (corresponding to the structural state of the membrane used for transport

measurements) and calculated according to the Equation (10) is ~ 29.5% and 12.6% for CTA and PBAT, respectively. These values well agree with the literature [45, 53, 54]. The DSC analysis of Aliquat 336 (not shown) did not exhibit a T_g, but revealed melting temperature at 19 °C in accordance with the reported literature value of 20 °C [55]. Comparing the curves of the obtained blend membranes with different polymer ratio with the curves of the pure polymers, one can notice that two T_g values are visible on the DSC curve for the 50CTA/50PBAT membrane at temperatures very close to the T_g values of pure polymers (Fig. 6). The presence of two distinct glass transitions of the 50CTA/50PBAT membrane indicates that the blend is immiscible, i.e. it behaves as the two-phase separated system. The total crystallinity of the 50CTA/50PBAT membrane was calculated as the sum of the crystallinity degree of both polymers taking into account their weight proportion (Eq. 10). This value is determined to be 14.9%.

In the case of BPIMs based on CTA/PBAT/30Aliquat 336 it was impossible to perform the DSC analysis at temperatures higher than 180 °C because of the thermal instability of Aliquat 336 (Fig. 5). However, one can easily observe the presence of the T_g value close to -37 °C which corresponds to the thermal transition of PBAT (Fig. 6). For the different CTA/PBAT membranes containing Aliquat 336, the T_g values of PBAT are slightly affected, maximum ~ 5 °C compared to the pure PBAT membrane. These small changes in the T_g values can be attributed to the partial miscibility of the low molar mass polymer chains. This phenomenon is not affected by the presence of the IL as the same changes are observed for the 50CTA/50PBAT membrane.

3.6. Wide angle X-ray diffraction (WAXD) analysis

The X-ray diffraction patterns of the obtained membranes (Fig. 7) are analyzed since the crystalline/amorphous ratio of the constituent polymer in a blend plays a very important role in the transport properties. The crystallinity of the membranes was calculated by the following equation:

$$X_{C_{WAXD}} = \frac{\Sigma A_{crystal}}{\Sigma A_{crystal} + \Sigma A_{amorph}} \cdot 100\% \qquad (11)$$

where $A_{crystal}$ and A_{amorph} are the fitted areas of the crystalline peaks and amorphous halos, respectively.

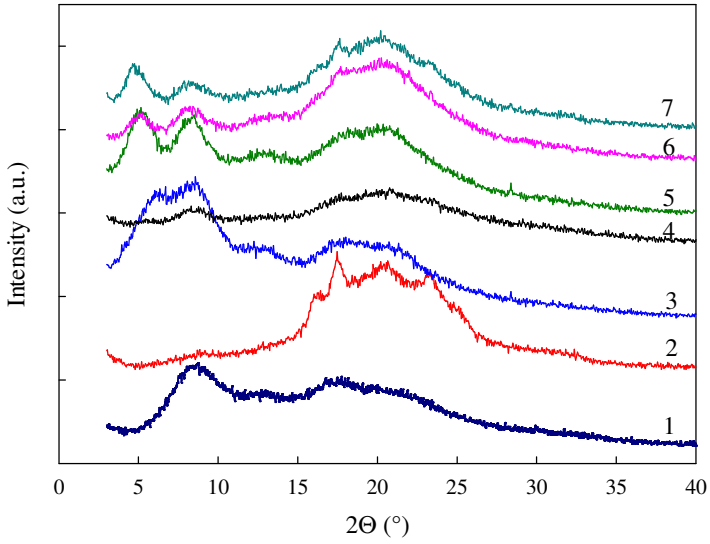

Figure 7. X-ray diffraction patterns of the obtained membranes: (*1*) CTA, (*2*) PBAT, (*3*) 70CTA/30Aliquat 336, (*4*) 50CTA/50PBAT, (*5*) 52.5CTA/17.5PBAT/30Aliquat 336, (*6*) 35CTA/35PBAT/30Aliquat 336, (*7*) 17.5CTA/52.5PBAT/30Aliquat 336.

The two main characteristic peaks of the pure CTA membrane observed at $2\theta = 8.5°$ and 17.4° (Fig. 7, curve 1) are referred to the crystalline and amorphous phases of CTA, respectively, and are in good agreement with the literature data [45]. The crystallinity degree obtained for the pure CTA membrane is equal to 30.2%, indicating that CTA is a semicrystalline polymer. This value is close to that found by the DSC analysis (29.5%). In the case of the pure PBAT membrane (Fig. 7, curve 2), five characteristic reflections at 16.3°, 17.5°, 20.5°, 23.1° and 25.0° are visible, corresponding to the planes of (011), (010), (110), (100), and (111), respectively, and indicating α-form triclinic packing of the PBAT molecules [52, 56]. The low intensity and broad shape of the diffraction reflections indicate a low crystallinity of PBAT (X_c = 13.6%). As in the case of the CTA membrane, the crystallinity degree obtained for the PBAT membrane is consistent with that calculated by DSC analysis (12.6%).

The X-ray diffraction pattern of the 70CTA/30Aliquat 336 membrane (Fig. 7, curve 3) is characterized by the higher peak intensity as well as the additional peak at 6.4° testifying to the fact that the addition of the ionic liquid to the membrane increases the membrane crystallinity. And really, the X_c value obtained in this case is equal to 49.8%. The presence of Aliquat 336 in the membrane structure facilitates the mobility of the CTA chains. Consequently, the CTA chains can assemble and form crystalline phases more easily. This

comes from the strong intermolecular and intramolecular hydrogen bonds in the CTA structure. This result also proves that Aliquat 336 plays a role of the plasticizer and is also in good agreement with the FTIR and mechanical analysis (Fig. 1 and 4, respectively). Lam et al. investigated the properties of the CTA-based membranes with different ionic liquids – 1-ethyl-3-methylimidazolium tetrafluoroborate ([emim][BF_4]) and 1-ethyl-3-methylimidazolium dicyanamide ([emim][dca]) [45]. The higher polymer chain mobility was noted in the presence of ionic liquid. Besides, it was found that [emim][dca] was slightly more effective than [emim][BF_4] in disrupting the CTA crystallization. However, at a higher ionic liquid content (i.e. more than 10 wt.%) the crystallization pic disappears because of the disruption of the hydrogen bonds among the -OH, esters, and ether oxygen groups, which is critical for the CTA chains in efficient packing and then crystallizing [45, 57]. As the increase of the crystallinity degree is observed in our case for the membrane with 30 wt.% ionic liquid compared to the pure CTA membrane (49.8% and 30.2%, respectively), it means that this content of Aliquat 336 is not sufficient to disrupt the CTA polymer chain crystallinity. Thus, one may conclude that the membrane crystallinity depends not only on the ionic liquid content, but also on the ionic liquid nature, i.e. the anion and cation groups.

In order to study the influence of the PBAT presence on the crystallization behavior of BPIMs, the membrane containing 50 wt.% CTA and 50 wt.% PBAT was obtained (50CTA/50PBAT) (Fig. 7, curve 4). The X-ray diffraction pattern of this membrane reveals the peaks of both polymers, i.e. CTA and PBAT. This fact means that the addition of PBAT does not change the crystalline structure but decreases the crystallinity of CTA up to 13.6% as the decrease in the intensity of the diffraction peaks is observed (Fig. 7, curve 4). This result can be explained by the ability of PBAT to alter the crystallinity of more crystalline polymers when it is mixed with them [31, 54].

The X-ray diffraction patterns of BPIMs reveal the appearance of new diffraction peak at about 5° (Fig. 7, curves 5-7). Taking into account that this peak is not present on the patterns of the pure polymers, 70CTA/30Aliquat 336 or 50CTA/50PBAT membranes, it can be attributed to the new crystalline structure appeared in the ternary membrane, containing CTA, PBAT and Aliquat 336. This result is also confirmed by the exothermic peak on the DSC curves of BPIMs (Fig. 6). As the interactions between the ionic liquid and polymers exist, Aliquat 336 may act as nucleating agent and the nucleation sites of a new crystalline structure in the CTA polymer may be formed [58]. Besides, the crystallinity values obtained for BPIMs containing different amount of PBAT confirm the PBAT ability to disrupt the CTA crystallization even in the presence of the ionic liquid. These results indicate that the

increasing of the proportion of PBAT in BPIMs affects the crystallinity of the membrane (X_c equals to 35.6%; 18.0% and 22.7% for 52.5CTA/17.5PBAT/30Aliquat 336, 35CTA/35PBAT/30Aliquat 336, and 17.5CTA/52.5PBAT/30Aliquat 336, respectively). Moreover, the higher is the PBAT content, the lower is the membrane crystallinity. It should be mentioned that the decrease of the membrane crystallinity can enhance the Cr(VI) transport performances as the solution diffusion occurs only in the polymer amorphous phases [59-61].

4. Transport properties

The membrane transport behavior is based on two phenomena: the diffusion caused by the chemical potential difference and the distribution of the substances between the membrane and aqueous phases. The chemical potential difference between the feed and the membrane is the first triggering force of the substance transport. Then, the substance penetrated from the feed solution to the membrane moves forward against diminishing the chemical potential difference between any two points in the membrane step by step. This phenomenon is known as extraction or removal and is expressed according to the Equation (6) as per cent extraction. All these phenomena are directly related to the facilitated diffusion.

In the aqueous solution the present species of the chromium are $Cr_2O_7^{2-}$, CrO_4^{2-}, $HCrO_4^-$ and $HCr_2O_7^-$. In highly acidic conditions (at pH < 0.5), chromium is rapidly protonated by hydronium ions and a stable chromic acid $H_2Cr_2O_7$ is formed. However, the chromic acid formation in the aqueous phase is not the desired situation during the chromium extraction process as the extraction of Cr(VI) ions decreases and thereby the flux and the permeability also decrease [62, 63]. Therefore, the solution with pH = 1 was chosen in the present study. It should be noted that Aliquat 336, quaternary ammonium chloride compound of main composition, trioctylmethyl ammonium chloride, represented as R_3CH_3NCl (R=C8 aliphatic) has been extensively used in the solvent extraction of anionic metal species. Its use as an ion-exchange extractant for chromium is based on the presence of extractable anionic chlorocomplexes of chromium that are ion-paired by the cation of the reagent, dissolved in a suitable solvent [64].

During the extraction following steps take place:

- chromium diffuses from the feed solution through PIM into the stripping solution due to the facilitated transport with Aliquat 336 acting as a carrier. The diffusion of ions in complex forming ion exchange is known to be proceeded by the "relay" mechanism [65]:

$$R_3CH_3N^+X^- + HCrO_4^- = R_3CH_3N^+HCrO_4^- + X^-$$

$$2(R_3CH_3N^+X^-)_m + CrO_4^{2-}{}_s = (R_3\ CH_3N^+)_2CrO_4^{2-}{}_{m,s} + 2Cl^-_s$$

where *m* is the membrane phase, *s* is the liquid phase (solution) and *m,s* is the membrane-solution interphase. At the beginning of the extraction the rate of the complex formation is rather high due to the availability of Aliquat 336 and also due to the very rapid diffusion assured by the continuous stirring of the solution;

- the apparent diffusion of the metal-extracting agent complex through PIM. The sorbed metal ions are transferred from the membrane surface to the Aliquat 336 molecules inside the membrane. This is the slowest stage of the process, since it is the transport of the adsorbed metal from the membrane surface inside PIM which controls the rate of the sorption process;
- the last third stage corresponds to the equilibrium state, represented by a plateau in the final part of the kinetic plot (Fig. 8a).

4.1. Influence of the membrane composition

To study the influence of the membrane composition on the Cr(VI) extraction, the measurements were performed for BPIMs with the different PBAT content in order to find the optimal membrane composition. The removal (Eq. 6), recovery (Eq. 7) and accumulation (Eq. 8) factors for all studied membranes as well as the calculated flux (Eq. 5) values are gathered in Table 2. It should be noted that previously performed transport measurements for the pure CTA and PBAT membranes (i.e. without Aliquat 336) didn't reveal any Cr(VI) removal.

Table 2. Transport performance of the obtained membranes.

Membrane	Removal factor, %	Recovery factor, %	Accumulation factor, %	Initial flux (μmol/(m²·s))
70CTA/30Aliquat 336	97.8±0.2	53.9±1.6	43.8±1.8	7.8±0.3
52.5CTA/17.5PBAT/30Aliquat 336	99.1±0.3	81.9±2.9	17.4±3.0	7.8±0.4
35CTA/35PBAT/30Aliquat 336	99.5±0.1	94.6±2.6	4.9±2.7	7.9±0.3
17.5CTA/52.5PBAT/30Aliquat 336	98.9±0.1	91.9±3.2	6.8±3.1	6.2±0.2

Fig. 8 presents the evolution of the Cr(VI) concentration in the feed and receiving phases as a function of time for each studied membrane. Cr(VI) was extracted successfully into all studied BPIMs. The decrease of the Cr(VI) concentration in the feed phase follows the same trend whatever the membrane composition (Fig. 8a) testifying to the same rate of the

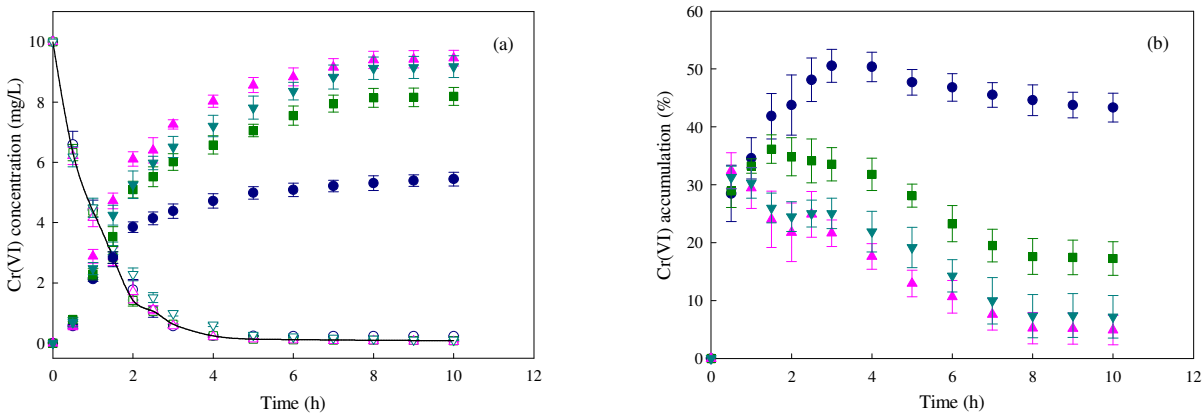

Figure 8. Time dependent changes in the Cr(VI) concentration in the feed (open symbols) and stripping (filled symbols) phases (*a*) and in the membrane phase (*b*):
(o) 70CTA/30Aliquat 336, (∈) 52.5CTA/17.5PBAT/30Aliquat 336,
(Δ) 35CTA/35PBAT/30Aliquat 336, (∇) 17.5CTA/52.5PBAT/30Aliquat 336
(pH 1, feed phase = 10 mg/L of Cr(VI) in 0.1 M HCl; stripping phase = 0.1 M NaOH).

Cr(VI) extraction. As one can see, initially the Cr(VI) concentration in the stripping phase increased rapidly and then some plateau value is reached whatever the membrane composition. However, the Cr(VI) transport is different depending on the membrane composition (Table 2 and Fig. 8). For example, for the 70CTA/30Aliquat 336 membrane the Cr(VI) concentration in the receiving phase increases rapidly during first two hours and then stays practically constant. The Cr(VI) concentration in the stripping phase reached equilibrium in around 6h for the 70CTA/30Aliquat 336 membrane and 8h – for CTA/PBAT/30Aliquat 336 membranes (Fig. 8a). In addition, the Cr(VI) concentration in the stripping phase is much higher in the case of the membranes containing PBAT compared to the pure CTA membrane (Fig. 8a).

At the same time, the flux value is practically the same whatever the membrane composition except for the membrane containing 52.5 wt.% PBAT, for which a slight decrease is observed (Table 2). This fact can be attributed to the membrane mechanical softness. Kebiche-Senhadji et al. observed the similar behavior for the membranes containing CTA, Aliquat 336 and NPOE with high plasticizer quantity (more than 30 wt.%) [26]. The permeability decrease in that case was explained by the limitation of the ion-pair movements of the Aliquat 336-Cr(VI) complex by the plasticization presence.

The recovery factor for the membrane without PBAT is only 53.9%, whereas this value reaches ~95% for the membrane containing 35 wt.% PBAT (Table 2). In addition, Fig. 8b shows that the accumulation factor is the lowest one for the membrane containing 35 wt.%

PBAT – only 4.9% in contrast to 43.8% in the case of the 70CTA/30Aliquat 336 membrane. As the recovery factor is a determinative factor for the transport experiments, this membrane composition (i.e. 35CTA/35PBAT/30Aliquat 336) is kept as an optimum.

Kozlowski and Walkowiak have demonstrated that for PIMs containing tri-*n*-octylamine (TOA) as a carrier and 2NPPE as a plasticizer, the carrier concentration has the main influence on the transport flux [63]. For example, the chromate ions are transported with the higher rate through the CTA-based membranes compared to the PVC-based membranes if the TOA concentration is less than 16 wt.%. However, the flux is comparable for both types of the membranes when the TOA concentration is higher than 16 wt.%. So, there exist some critical value of the plasticizer concertation starting from which the water contact angle values for the membranes are rather similar, i.e. there is no influence of the membrane composition on the membrane hydrophilic character. As in our case the water contact angle values for studied BPIMs are close enough whatever the PBAT content in the membrane (Fig. 2), i.e. the membranes possess the same hydrophilicity level, that's why the practically similar values of flux were obtained (Table 2).

The Cr(VI) accumulation (i.e. the membrane capacity) is the metal quantity retained inside the membrane. The Cr(VI) amount inside the membrane rises at the beginning to attain a maximum (47-55% depending on the membrane composition) after approximately 2.5h of transport and decreases slowly corresponding to the progress of the Cr(VI) discharge into the stripping phase (Fig. 8b), thus allows obtaining the Cr(VI) extraction from the feed solution to the stripping phase. This result is comparable to that reported by Kavitha and Palanivelu [66]. They observed a maximum of 11% of the Cu(II) retention inside a PIM membrane containing di(2-ethylhexyl) phosphoric acid as a carrier, CTA as a polymer matrix and di-octyl phthalate as a plasticizer.

In the case of the PBAT-free membrane (i.e. 70CTA/30Aliquat 336), the high concentration of the accumulated Cr(VI) (~44%) was observed even after 10h (Fig. 8b). Such behavior may be explained by the fact that the quantity of chromium entering into the membrane (i.e. removal) is much higher than the chromium quantity which is moving to the stripping phase (i.e. recovery). Indeed, the CTA-based membranes require the presence of an additional plasticizer in order to improve both the transport performance and the compatibility between the membrane components [26, 67] or the use of a carrier of high quantity (often more than 40%) [21, 23].

The obtained enhancement of the Cr(VI) transport performance (Table 2) is attributed to the incorporation of the flexible PBAT macromolecular chains into the rigid CTA

membrane. In this case, a membrane with new physico-chemical properties different from those of the 70CTA/30Aliquat 336 membrane is obtained. As it is shown by the mechanical measurements (Fig. 4), the PBAT addition makes the membranes more flexible as their stiffness decreases. So, one can say that PBAT acts as a plasticizer. The higher flexibility of the polymer chains results in the lower diffusive resistance to the mass transfer of the Aliquat-Cr(VI) ion-pairs within the membrane. Also, the Aliquat 336-Cr(VI) ion-pairs may have a higher compatibility with PBAT compared to CTA. Kebiche-Senhadji et al. studied the Cr(VI) extraction performance of PIMs based on CTA and different content of Aliquat 336 [26]. It was found that the percolation was reached for the membrane with 14.4 wt.% of Aliquat 336. However, the optimal permeability was reached in the case of the membrane with ~57% of Aliquat 336 and 30% of NPOE, thus testifying to the necessity to use the high quantity of carrier and plasticizer in order to ensure sufficient transport properties. Almeida et al. studied the influence the chemical nature of plasticizers on the membrane Cr(VI) extraction properties [18]. They found that the highest Cr(VI) recovery factor (88%) was obtained in the presence of NPOE, while only 50% and 32% of the Cr(VI) ions are recovered using dibutyl phthalate and 2-fluorophenyl 2-nitrophenyl ether, respectively. Such result was explained by the plasticizer viscosity and its dielectric constant. In any case, the high amount of plasticizer should be used in those membranes (more than 30 wt.%).

The other reason why the recovery ability increases for the membranes containing PBAT is the decrease of the crystallinity value with the PBAT addition as the diffusion of the Aliquat 336 – Cr(VI) complex occurs only through the polymer amorphous phase. And really, the membrane with the lowest crystallinity degree (18.0%), i.e. 35CTA/35PBAT/30Aliquat 336, has the best extraction performance.

4.2. Membrane stability

Repeated cycles of the Cr(VI) extraction were carried out using the same membrane in order to compare the stability of the 70CTA/30Aliquat 336 and 35CTA/35PBAT/30Aliquat 336 membranes. The stability measurement was performed during 128h by refreshing the feed and stripping phases at the end of each cycle (8h). Fig. 9a shows the evolution of the recovery factor (Eq. 7) for each extraction experiment over 16 cycles for the 35CTA/35PBAT/30Aliquat 336 membrane and over 5 cycles for the 70CTA/30Aliquat 336 membrane. One can see that both membranes gradually lose extraction efficiency. The stability of the CTA-based membranes during the extraction process has been already studied by several authors [19, 26, 63]. Kaya et al. revealed that the Cr(VI) removal factor was

reduced up to 60% after ten cycles (cycle duration is 6h) for the CTA/Aliquat 336 membrane with calix[4]arene as a carrier [19].

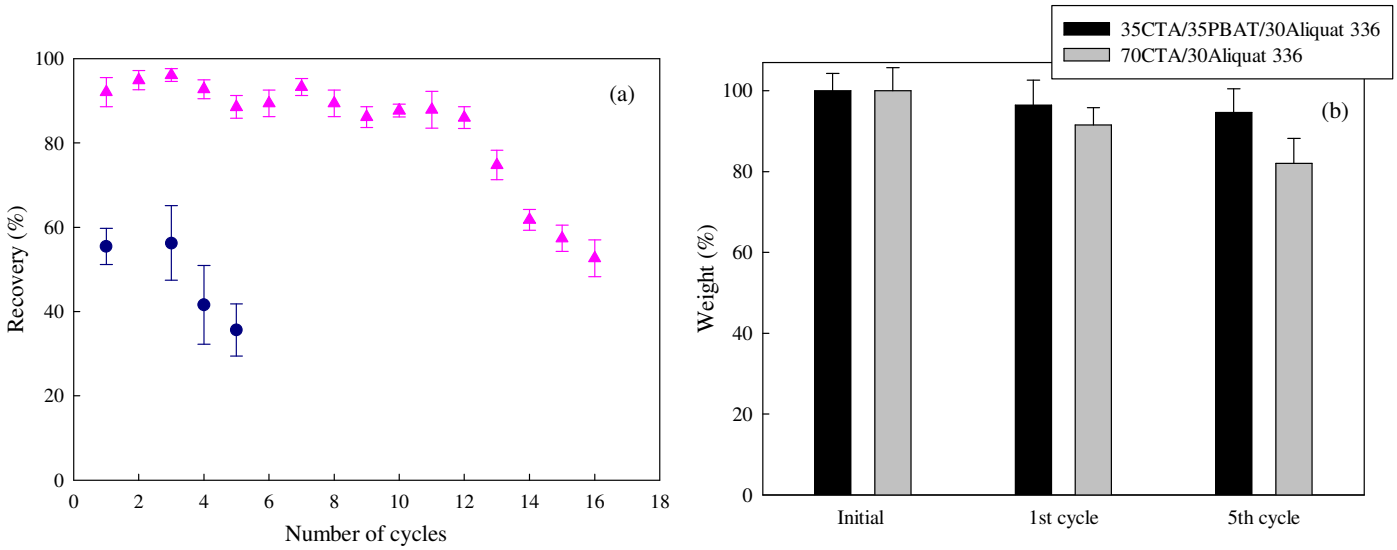

Figure 9. (*a*) Membrane recovery efficiency as a function of the number of measurements: (o) 70CTA/30Aliquat 336 and (Δ) 35CTA/35PBAT/30Aliquat 336 (pH 1, feed phase = 10 mg/L of Cr(VI) in 0.1 M HCl; stripping phase = 0.1 M NaOH); (*b*) Membrane weight as a function of the number of measurements.

The extraction efficiency for the 35CTA/35PBAT/30Aliquat 336 membrane is relatively stable up to 12 cycles (Fig. 9a). So, it can be concluded that this membrane has acceptable stability till 12 cycles (the cycle duration is 8h). The extraction improvement for this membrane can be explained by the fact that the mixture of the flexible PBAT polymer chains with the CTA chains allows better entangling the ionic liquid as the increased tortuosity is observed. Therefore, Aliquat 336 is better retained inside the membrane, thus limiting its loss into the aqueous phase. In order to check this explanation, the thermal analysis of membranes and their weighing (Fig. 9b) were performed after each extraction cycle. The quantity of Aliquat 336 remains close to 28% and 21% after one cycle for the 35CTA/35PBAT/30Aliquat 336 and 70CTA/30Aliquat 336 membranes, respectively. Further reduction of the Aliquat 336 content is observed with the extraction cycles increase, i.e. to about 12% for the 70CTA/30Aliquat 336 membrane after 5 cycles and to 20% for the 35CTA/35PBAT/30Aliquat 336 membrane after 16 cycles. However, in any case the higher ionic liquid retention is observed for the membrane containing PBAT. This result is in good agreement with the membrane weight loss measurements (Fig. 9b). For clarity, the weight of the fresh membrane (i.e. before the extraction study) was assumed to be 100%. A significant weight loss is noticed for the 70CTA/30Aliquat 336 membrane, namely about 9% after one

cycle and ca. 18% after 5 cycles. The higher stability is revealed for the 35CTA/35PBAT/30Aliquat 336 membrane, namely, less than 6% after 5 cycles of extraction. Thus, the main reason of the efficiency loss is the leaching of Aliquat 336 from the membrane into the aqueous phase. Also, the Cr(VI) ions remaining in the membrane may affect subsequent extraction measurements since the membrane becomes yellow only after one cycle of extraction. Moreover, it should be noted that the thickness of the 35CTA/35PBAT/30Aliquat 336 membrane was practically stable up to 7 cycles, but after 16 extraction cycles it decreased considerably – from ~110 µm up to ~58 µm. This decrease is caused by the chemical degradation of the membrane as it stays in rather aggressive media, i.e. highly acidic and basic media on each membrane side. This phenomenon can also provoke the deterioration of the membrane transport performance. Thus, it would be interesting to study the Cr(VI) extraction efficiency in mild conditions.

4.3. Membrane selectivity

The selectivity is a very significant factor for the development and industrial application of PIMs due to the environmental process. To investigate the selectivity of the obtained membrane with the optimum composition, the extraction measurements were performed in the presence of Cr(VI), Fe(III), Co(II), Cd(II), Zn(II), Pb(II), Ni(II) and Cu(II) metal ions in the initial feed phase (0.1 M HCl). The stripping phase was 0.1 M NaOH as in previous transport study. The obtained results are presented in Fig. 10. After 10h of the

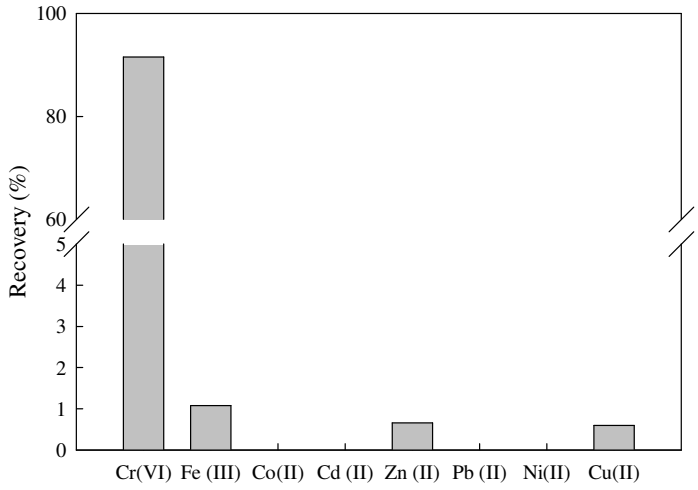

Figure 10. Influence of the type of interfering ions on the Cr(VI) recovery capacity for the 35CTA/35PBAT/30Aliquat 336 membrane
(pH 1, feed phase = 10 mg/L of metal ions in 0.1 M HCl; stripping phase = 0.1 M NaOH).

extraction process, Cr(VI) was transported successfully to the stripping phase with a recovery factor of 91.5%. One can conclude that the membrane composed of CTA, PBAT and Aliquat 336 reveals a great selectivity to Cr(VI) ions. No recovery for Co(II), Cd(II), Pb(II) and Ni(II) was observed and the recovery less than 1% was detected for Fe(III), Zn(II) and Cu(II). Consequently, the membrane containing PBAT can be tested on real samples.

Conclusion

New BPIMs based on CTA and Aliquat 336 were successfully obtained using biodegradable polymer – PBAT. The FTIR analysis results revealed the presence of the interactions between the negatively charged carboxyl groups of CTA and the positively charged ammonium groups of Aliquat 336 and between the hydroxyl groups of CTA and the carboxyl groups of PBAT. The SEM study confirmed the absence of pores in the obtained membranes at µm scale. The water contact angle measurements revealed that the studied BPIMs are very hydrophilic (~22°) whatever the PBAT content. In addition, the crystallinity degree was found to decrease significantly from 49.8% for the 70CTA/30Aliquat 336 membrane to 18.0% for the 35CTA/35PBAT/30Aliquat 336 membrane. The transport experiments were performed to examine the ability of the obtained membranes based on CTA, PBAT and Aliquat 336 to extract Cr(VI) ions. It was observed that BPIMs containing PBAT prepared in this study were more effective regarding the transport of Cr(VI) from the feed solution to the stripping solution. The membranes based on CTA and Aliquat 336 with only 17.5 wt.% PBAT accumulate a high amount of Cr(VI). However, with the increase of the PBAT content in the membrane composition, the Cr(VI) accumulation in the membrane phase decreases and the recovery factor increases. It was determined that the transport of Cr(VI) was the highest when the membrane contained 35 wt.% PBAT, 35 wt.% CTA and 30 wt.% Aliquat 336. It was possible to re-use the same membrane for repeated transport experiments. The presence of PBAT in the membrane minimized carrier loss, thus providing superior stability compared to the corresponding membrane containing only CTA and Aliquat 336. The stability of that membrane was constant for 12 cycles and each cycle run was carried out for 8h. However, some degree of deterioration in the extraction performance was still observed for the CTA/PBAT/Aliquat 336 membrane over 12 consecutive transport measurements.

The obtained membrane has the selectivity to separate Cr(VI) from the solution in the presence of other heavy metal ions (Fe(III), Co(II), Cd(II), Zn(II), Pb(II), Ni(II) and Cu(II)).

Thus, it is found that the introduction of PBAT into the CTA/Aliquat 336-based membrane is successful and can be used for the Cr(VI) recovery.

The obtained results reveal that addition of PBAT into the CTA-based membranes improves strongly both the membrane efficiency and stability in comparison with the traditional CTA-based membranes. In particular, the 35CTA/35PBAT/30Aliquat 336 membrane appears as a promising PIM for the Cr(VI) removal of from aqueous solutions.

Acknowledgement

F. Sellami acknowledges the University of Bejaia (Alegia) and Algerian Government for the financial support for his PhD thesis (Short-term Scientific internship and PNE 2016-2017).

Data availability

The raw/processed data required to reproduce these findings cannot be shared at this time as the data also forms part of an ongoing study.

References

1. W. Ni, Y. Huang, X. Wang, J. Zhang, K. Wu, Associations of neonatal lead, cadmium, chromium and nickel co-exposure with DNA oxidative damage in an electronic waste recycling town // Sci. Total Environ. 472 (2014) 354–362.

2. A.H. Stern, A quantitative assessment of the carcinogenicity of hexavalent chromium by the oral route and its relevance to human exposure // Environ. Res. 110 (2010) 798–807.

3. J. Chen, W.G. Thilly, Mutational spectrum of chromium(VI) in human cells // Mutat. Res. 323 (1994) 21–27.

4. S.A. Jabasingh, D. Lalith, P. Garre, Sorption of chromium(VI) from electroplating effluent onto chitin immobilized mucor racemosus sorbent (CIMRS) impregnated in rotating disk contactor blades // J. Ind. Eng. Chem. 23 (2015) 79–92.

5. S. Meriç, E. De Nicola, M. Iaccarino, M. Gallo, A. Di Gennaro, G. Morrone, et al., Toxicity of leather tanning wastewater effluents in sea urchin early development and in marine microalgae // Chemosphere 61 (2005) 208–217.

6. D. Cetin, S. Dönmez, G. Dönmez, The treatment of textile wastewater including chromium(VI) and reactive dye by sulfate-reducing bacterial enrichment // J. Environ. Manag. 88 (2008) 76–82.

7. N.E. El-Hefny, Comparison of liquid–liquid extraction of Cr(VI) from acidic and alkaline solutions by two different amine extractants // Sep. Purif. Technol. 67 (2009) 44–49.
8. A.K. Golder, A.K. Chanda, A.N. Samanta, S. Ray, Removal of hexavalent chromium by electrochemical reduction–precipitation: investigation of process performance and reaction stoichiometry // Sep. Purif. Technol. 76 (2011) 345–350.
9. Y.S. Dzyazko, A.S. Rudenko, Y.M. Yukhin, A.V. Palchik, V.N. Belyakov, Modification of ceramic membranes with inorganic sorbents. Application to electrodialytic recovery of Cr(VI) anions from multicomponent solution // Desalination 342 (2014) 52–60.
10. M. Kebir, M. Trari, R. Maachi, N. Nasrallah, B. Bellal, A. Amrane, Relevance of a hybrid process coupling adsorption and visible light photocatalysis involving a new hetero-system $CuCo_2O_4/TiO_2$ for the removal of hexavalent chromium // J. Environ. Chem. Eng. 3 (2015) 548–559.
11. P. Venkateswaran, K. Palanivelu, Studies on recovery of hexavalent chromium from plating wastewater by supported liquid membrane using tri-*n*-butyl phosphate as carrier // Hydrometallurgy 78 (2005) 107–115.
12. A. Benjjar, T. Eljaddi, O. Kamal, K. Touaj, L. Lebrun, M. Hlaibi, The development of new supported liquid membranes (SLMs) with agents: methyl cholate and resorcinarene as carriers for the removal of dichromate ions ($Cr_2O_7^{2-}$) // J. Environ. Chem. Eng. 2 (2014) 503–509.
13. C. Jung, J. Heo, J. Han, N. Her, S.-J. Lee, J. Oh, J. Ryu, Y. Yoon, Hexavalent chromium removal by various adsorbents: powdered activated carbon, chitosan, and single/multi-walled carbon nanotubes // Sep. Purif. Technol. 106 (2013) 63–71.
14. K. Scott, Handbook of industrial membranes. Kidlington: Elsevier, 1997.
15. Y. Yildiz, A. Manzak, B. Aydýn, O. Tutkun, Preparation and application of polymer inclusion membranes (PIMs) including alamine 336 for the extraction of metals from an aqueous solution // Mater. Technol. 48 (2014) 791–796.
16. Y.Y. Bonggotgetsakul, M. Ashokkumar, R.W. Cattrall, S.D. Kolev, The use of sonication to increase extraction rate in polymer inclusion membranes: an application to the extraction of gold (III) // J. Membr. Sci. 365 (2010) 242–247.
17. L. Nghiem, P. Mornane, I. Potter, J. Perera, R.W. Cattrall, S.D. Kolev, Extraction and transport of metal ions and small organic compounds using polymer inclusion membranes (PIMs) // J. Membr. Sci. 281 (2006) 7–41.

18. M.I.G.S. Almeida, R.W. Cattrall, S.D. Kolev, Recent trends in extraction and transport of metal ions using polymer inclusion membranes (PIMs) // J. Membr. Sci. 415–416 (2012) 9–23.

19. A. Kaya, C. Onac, H. Korkmaz Alpoguz, A. Yilmaz, N. Atar, Removal of Cr(VI) through calixarene based polymer inclusion membrane from chrome plating bath water // Chem. Eng. J. 283 (2016) 141–149.

20. M. Resina, C. Fontas, C. Palet, M. Munoz, Comparative study of hybrid and activated composite membranes containing Aliquat 336 for the transport of Pt(IV) // J. Membr. Sci. 311 (2008) 235–242.

21. R. Güell, E. Anticó, S.D. Kolev, J. Benavente, V. Salvadó, C. Fontàs, Development and characterization of polymer inclusion membranes for the separation and speciation of inorganic As species // J. Membr. Sci. 383 (2011) 88–95.

22. A. Stojanovic, B.K. Keppler, Ionic liquids as extracting agents for heavy metals // Sep. Sci. Technol. 47 (2012) 189–203.

23. I. Vázquez, V. Romero, C. Fontàs, E. Anticó, J. Benavente, Polymer inclusion membranes (PIMs) with the ionic liquid (IL) Aliquat 336 as extractant: effect of base polymer and IL concentration on their physical–chemical and elastic characteristics // J. Membr. Sci. 455 (2014) 312–319.

24. A.L. Ocampo, J.C. Aguilar, E.R.D. Miguel, M. Monroy, P. Roquero, J. de Gyves, Novel proton-conducting polymer inclusion membranes // J. Membr. Sci. 326 (2009) 382–387.

25. J.S. Gardner, J.O. Walker, J.D. Lamb, Permeability and durability effects of cellulose polymer variation in polymer inclusion membranes // J. Membr. Sci. 229 (2004) 87–93.

26. O. Kebiche-Senhadji, S. Tingry, P. Seta, M. Benamor, Selective extraction of Cr(VI) over metallic species by polymer inclusion membrane (PIM) using anion (Aliquat 336) as carrier // Desalination 258 (2010) 59–65.

27. G. Crini, Recent developments in polysaccharide-based materials used as adsorbents in wastewater treatment // Prog. Polym. Sci. 30 (2005) 38–70.

28. R. Ahmad, I. Hasan, L-methionine montmorillonite encapsulated guar gum-g-polyacrylonitrile copolymer blend hybrid nanocomposite for removal of heavy metals // Ground. Sustain. Develop. 5 (2017) 75-84.

29. F.C. Wu, R.L. Tseng, R.S. Juang, A review and experimental verification of using chitosan and its derivatives as adsorbents for selected heavy metals // J. Environ. Manag. 91 (2010) 798–806.

30. S.S. Ray, Environmentally friendly polymer nanocomposites. Philadelphia: Woodhead Publishing, 2013.
31. C.-S. Wu, Characterization of cellulose acetate-reinforced aliphatic–aromatic copolyester composites // Carbohydr. Polym. 87 (2012) 1249–1256.
32. K. Annane, A. Sahmoune, P. Montels, S. Tingry, Polymer inclusion membrane extraction of cadmium(II) with Aliquat 336 in micro-channel cell // Chem. Eng. Res. Des. 94 (2015) 605–610.
33. D.A. Cerqueira, G.R. Filho, R.M.N. Assuncao, A new value for the heat of fusion of a perfect crystal of cellulose acetate // Polym. Bul. 56 (2006) 475-482.
34. P. R. Danesi, Separation of metal species by supported liquid membranes // Sep. Sci. Technol. 19 (1984) 857-894.
35. O. Arous, H. Kerdjoudj, P. Seta, Comparison of carrier-facilitated silver (i) and copper (ii) ions transport mechanisms in a supported liquid membrane and in a plasticized cellulose triacetate membrane // J. Membr. Sci. 241 (2004) 177–185.
36. O. Kebiche-Senhadji, L. Mansouri, S. Tingry, P. Seta, M. Benamor, Facilitated Cd(II) transport across CTA polymer inclusion membrane using anion (Aliquat 336) and cation (D2EHPA) metal carriers // J. Membr. Sci. 310 (2008) 438–445.
37. B.V.M. Rodrigues, A.S. Silva, G.F.S. Melo, L.M.R. Vasconscellos, F.R. Marciano, A.O. Lobo, Influence of low contents of superhydrophilic MWCNT on the properties and cell viability of electrospun poly(butylene adipate-*co*-terephthalate) fibers // Mater. Sci. Eng. C 59 (2016) 782–779.
38. Y.-X. Weng, Y.-J. Jin, Q.-Y. Meng, L. Wang, M. Zhang,Y.-Z. Wang, Biodegradation behavior of poly(butylene adipate-*co*-terephthalate) (PBAT), poly(lactic acid) (PLA), and their blend under soil conditions // Polym. Test. 32 (2013) 918-926.
39. J.P. Mikkola, P. Virtanen, R. Sjöholm, Aliquat 336 – a versatile and affordable cation source for an entirely new family of hydrophobic ionic liquids // Green Chem. 8 (2006) 250–255.
40. H. Cui, J. Chen, H. Yang, W. Wang, Y. Liu, D. Zou, W. Liu, G. Men, Preparation and application of Aliquat 336 functionalized chitosan adsorbent for the removal of Pb(II) // Chem. Eng. J. 232 (2013) 372–379.
41. O. Kebiche-Senhadji, S. Bey, G. Clarizia, L. Mansouri, M. Benamor, Gas permeation behavior of CTA polymer inclusion membrane (PIM) containing an acidic carrier for metal recovery (DEHPA) // Sep. Purif. Technol. 80 (2011) 38-44.

42. S.K. Shalu, R.K. Chaurasia, R.K. Singh, S. Chandra, Thermal stability, complexing behavior, and ionic transport of polymeric gel membranes based on polymer PVdF-HFP and ionic liquid, [BMIM][BF_4] // J. Phys. Chem. B 117 (2013) 897-906.
43. L. Liang, Q. Gan, P. Nancarrow, Composite ionic liquid and polymer membranes for gas separation at elevated temperatures // J. Membr. Sci. 450 (2014) 407–417.
44. L.N. Sim, S.R. Majid, A.K. Arof, Effects of 1-butyl-3-methyl imidazolium trifluoromethanesulfonate ionic liquid in poly(ethyl methacrylate)/poly(vinylidenefluoride-*co*-hexafluoropropylene) blend based polymer electrolyte system // Electrochim. Acta 123 (2014) 190–197.
45. B. Lam, M. Wei, L. Zhu, S. Luo, R. Guo, A. Morisato, P. Alexandridis, H. Lin, Cellulose triacetate doped with ionic liquids for membrane gas separation // Polymer 89 (2016) 1-11.
46. H.I. Turgut, V. Eyupoglu, R.A. Kumbasar, I. Sisman, Alkyl chain length dependent Cr(VI) transport by polymer inclusion membrane using room temperature ionic liquids as carrier and PVDF-*co*-HFP as polymer matrix // Sep. Pur. Technol. 175 (2017) 406-417.
47. I. Iben Nasser, F. Ibn El Haj Amor, L. Donato, C. Algieri, A. Garofalo, E. Drioli, C. Ahmed, Removal and recovery of $Ag(CN)_2^-$ from synthetic electroplating baths by polymer inclusion membrane containing Aliquat 336 as a carrier // Chem. Eng. J. 295 (2016) 207-217.
48. T. Uesaka, K. Nakane, S. Maeda, T. Ogihara, N. Ogata, Structure and physical properties of poly(butylene succinate)/cellulose acetate blends // Polymer 41 (2000) 88449-8454.
49. F.B.M. Suah, M. Ahmad, Preparation and characterization of polymer inclusion membrane based optode for determination of Al^{3+} ion // Anal. Chim. Acta 951 (2017) 133-139.
50. K. Hamad, M. Kaseem, F. Deri, Y.G. Ko, Mechanical properties and compatibility of polylactic acid/polystyrene polymer blend // Mater. Let. 164 (2016) 4409-412.
51. S. Rajesh, P. Maheswari, S. Senthilkumar, A. Jayalakshmi, D. Mohan, Preparation and characterisation of poly (amide-imide) incorporated cellulose acetate membranes for polymer enhanced ultrafiltration of metal ions // Chem. Eng. J. 171 (2011) 33-44.
52. F. Chivrac, Z. Kadlecová, E. Pollet, L. Avérous, Aromatic copolyester-based nanobiocomposites: elaboration, structural characterization and properties // J. Polym. Environ. 14 (2006) 393-401.
53. G. Li, S. Shankar, J.-W. Rhim, B.-Y. Oh, Effects of preparation method on properties of poly(butylene adipate-*co*-terephthalate) films // Food Sci. Biotechnol. 24 (2015) 1679-1685.

54. S. Dhandapani, S.K. Nayak, S. Mohanty, Investigation of miscibility, crystallinity and phase morphology of a novel bio based poly(trimethylene terephthalate)/poly(butylene adipate-*co*-terephthalate) bland //Polym. Sci. Ser. A 57 (2015) 783-791.

55. J.-P. Mikkola, P. Virtanen, R. Sjoholm, Aliquat 336® – a versatile and affordable cation source for an entirely new family of hydrophobic ionic liquids // Green Chem. 8 (2006) 250-255.

56. X.Q. Shi, H. Ito, T. Kikutani, Characterization on mixed-crystal structure and properties of poly(butylene adipate-co-terephthalate) biodegradable fibers // Polymer 46 (2005) 11442-11450.

57. M. FitzPatrick, P. Champagne, M.F. Cunningham, The effect of subcritical carbon dioxide on the dissolution of cellulose in the ionic qliuid 1-ethyl-3-methylimidazolium acetate // Cellulose 19 (2012) 37-44.

58. L.C. Lins, S. Livi, J. Duchet-Rumeau, J.-F. Gérard, Phosphonium ionic liquds as new compatibilizing agents of biopolymer blends composed of poly(butylene-adipate-*co*-terephtalate)/poly(lactic acid) (PBAT/PLA) // RSC Adv. 5 (2015) 59082-59092.

59. B.S. Lalia, V. Kochkodan, R. Hashaikeh, N. Hilal, A review on membrane fabrication: structure, properties and performance relationship // Desalination 326 (2013) 77-95.

60. J.G.A. Bitter, Effect of crystallinity and swelling on the permeability and selectivity of polymer membranes // Desalination 51 (1984) 19-35.

61. K. Friess, J.C. Jansen, F. Bazzarelli, P. Izak, V. Jarmarova, M. Kacirkova, J. Schauer, G. Clarizia, P. Bernardo, High ionic liquid content polymeric gel membranes: correlation of membrane structure with gas and vapour transport properties // J. Membr. Sci. 415-416 (2012) 801-809.

62. V. Eyupoglu, O. Tutkun, The extraction of Cr(VI) by a flat sheet supported liquid membrane using Alamine 336 as a carrier // Arab J. Sci. Eng. 36 (2011) 529-539.

63. C.A. Kozlowski, W. Walkowiak, Applicability of liquid membranes in chromium (VI) transport with amines as ions carriers // J. Membr. Sci. 266 (2005) 143-150.

64. P. Loyson, The solvent extraction of zinc from lithium chloride by Aliquat 336 chloride, bromide and iodide in chloroform: an analytical investigation // Solv. Extract. Ion Exch. 18 (2000) 25-39.

65. V.D. Kopylova, Complexation in ion exchange phase. Properties and application of ion exchanger complexes, Solv. Extract. Ion Exch. 16 (1998) 267-343.

66. N. Kavitha, K. Palanivelu, Recovery of copper (II) through polymer inclusion membrane with di(2-ethylhexyl) phosphoric acid as carrier from e-waste // J. Membr. Sci. 415-416 (2012) 663-669.
67. S.P. Best, S.D. Kolev, J.R.P. Gabriel, R.W. Cattrall, Polymerization effects in the extraction of Co(II) into polymer inclusion membranes containing Cyanex 272. Structural studies of the Cyanex 272 – Co(II) complex // J. Membr. Sci. 497 (2016) 377-386.